J. Kor. Soc. Fish. Tech., 46 (1), 070 - 081, 2010
DOI:10.3796/KSFT.2010.46.1.070

FISHERIES TECHNOLOGY
www.fishtech.or.kr

Analytical study of house wall and air temperature transients under on-off and proportional control for different wall type

Kyu-Il HAN*

Division of Mechanical System Engineering, School of Mechanical Engineering, Pukyong National University, Busan 608-739, Korea

A mathematical model is formulated to study the effect of wall mass on the thermal performance of four different houses of different construction. This analytical study was motivated by the experimental work of Burch et al. An analytical solution of one -dimensional, linear, partial differential equation for wall temperature profiles and room air temperatures is obtained using the Laplace transform method. Typical Meteorological Year data are processed to yield hourly average monthly values. These discrete data are then converted to a continuous, time dependent form using a Fast Fourier Transform method. This study is conducted using weather data from four different locations in the United States: Albuquerque, New mexico; Miami, Florida; Santa Maria, California; and Washington D.C. for both winter and summer conditions. A computer code is developed to calculate the wall temperature profile, room air temperature, and energy consumption loads. Three sets of results are calculated one for no auxiliary energy and two for different control mechanism -- an on-off controller and a proportional controller. Comparisons are made for the cases of two controllers. Heavy weight houses with insulation in mild weather areas (such as August in Santa Maria, California) show a high comfort level. Houses using proportional control experience a higher comfort level in comparison to houses using on-off control. The result shows that there is an effect of mass on the thermal performance of a heavily constructed house in mild weather conditions.

Key words: Thermal mass, On-off controller, Proportional controller, Energy consumption load

Introduction

Much attention has been focused on strategies for reducing energy consumption in residential, commercial and industrial buildings due to rapidly rising costs of heating and cooling. A great deal of work has been done and many methods have been developed to obtain energy consumption loads for buildings. Some works (Mitalas et al., 1967, 1968) use the transfer function approach for calculating energy loads. This concept is first introduced by them using what they call room thermal response factors.

The study done by Zabinski et al. (1974) focuses on heat losses based on the indoor-outdoor

*Corresponding author: kihan@pknu.ac.kr, Tel: 82-51-629-6194, Fax: 82-51-629-6180

temperature difference and investigates the effect of varied thermostat settings on fuel consumption. Their results show that lowering the set-point temperature overnight saves fuel.

Crall et al. (1995) use computer simulation to calculate building heating load. The results of this study clearly demonstrate that it is possible, given certain basic data on a building and the details of its environmental control system, to determine accurately the energy requirements for heating and cooling.

A computer model for simulating heat flow by conduction through walls and roofs is developed based on the transmission matrix method (Buffington, 1995). The transmission matrix method relates the periodic temperature and heat flux on one side of a homogeneous layer to the periodic temperature and heat flux on the other side by means of a transmission matrix. The main advantage of the transmission matrix method is the simplicity with which the model describes transient inside air temperatures.

Articles (Burch et al., 1984, Hopkins et al., 1979, Rudoy et al., 1979) investigate which construction materials consume less energy under varying climatic conditions. It has been postulated that, as mass is added to the building envelope, the thermal resistances of the building envelope can be reduced without changing annual heating requirements of the building (Goodwin et al., 1979). Mass is more effective in reducing heating requirements for buildings located in warmer areas where the heat loss relative to the heat gain is low. The mass effect also decreases cooling loads.

Similar results are obtained by Burch et al. (1984). His group recently conducted experiments on six test buildings in Gaithersburg, MO. These buildings were instrumented to measure heating and cooling loads, and indoor comfort. They focus on the effect of different construction materials in determining the energy consumption load.

All of these studies are deficient in one or more ways. The experimental studies exhibit a very small savings due to mass, of the same magnitude as the effect of solar radiation absorbed by and transmitted through the walls. The analytical studies do not include a realistic model of the energy plant.

The main purpose of this study is to develop a method from a rigorous mathematical basis to analyze the wall temperature profile, the room air temperature, the energy consumption load, and the comfort level. The scope will include both heating and cooling. This study also investigates two widely used controllers (i.e. the on-off controller and the proportional controller) to assess the effect upon energy consumption.

Theoretical formulation

The formulation of an analytical method for obtaining wall temperature profile, room air temperature and energy consumption load is presented.

Four of the six houses studied by Burch et al. are modelled. Each test house is a 6.1m by 6.1m by 2.3m one-room house. The houses have identical floor plans and orientations and are identical except for wall construction, which is as follows: insulated lightweight wood frame; insulated masonry with outside mass; uninsulated masonry; and insulated masonry with inside mass. The details of the wall construction for each of the four houses are presented in Table 1.

Weather data for four cities in the United States are used in this study. Twenty-four discrete data points calculated from TMY (Typical Meteorological Year) weather data files (1998) are converted to

Table 1. Wall construction types

#1 : Insulated lightweight wood frame
13mm (0.5 in) gypsum board
0.05mm (0.002 in) polyethylene film
50 × 100 mm (2 × 4 in) studs placed 410 mm (16 in) o.c. with R-11 16 mm (5/8 in) exterior plywood
#2 : Insulated masonry (outside mass)
13mm (0.5 in) gypsum board
0.05mm (0.002 in) polyethylene film
51 mm (2 in) thick extruded polystyrene insulation placed between 38 mm (1-1/2 in) wide wood furring strips placed 610 mm (24 in) o.c.
6.4 mm (1/4 in) air space
100mm (4 in) 2-core hollow concrete block 1680 kg/m^3 (105 lb/ft^3)
100 mm (4 in) face brick
#3 : Uninsulated masonry
13mm (0.5 in) gypsum board
0.05mm (0.002 in) polyethylene film
20 mm (3/4 in) air space created by 50 × 20 mm (2 × 3/4 in) furring strips placed 410 mm (16 in) o.c.
200 mm (8 in) 2-core hollow concrete block 1680 kg/m^3 (105 lb/ft^3)
#4 : Insulated masonry (inside mass)
13 mm (0.5 in) plaster
200 mm (8 in) 2-core hollow concrete block 1680 kg/m^3 (105 lb/ft^3)
89mm (3-1/2 in) perlite insulation in space between block and brick
100 mm (4 in) face brick

continuous form via a Fast Fourier Transform. Each house is modelled by a single homogeneous wall and an air node. Two types of control functions (i.e. an on-off controller and a proportional controller) are presented.

The thermal system is represented mathematically by two energy balances: one on the wall, and the other on the room air. The equation for the wall temperature distribution is derived using Fourier's law of heat conduction. The case studied represents a linear flow of heat in a solid wall bounded by a pair of parallel planes, at x = 0 and x = L.

There may, in reality, be significant heat transfer through the building's roof and floor. However to render the problem amenable to analysis, it is assumed that a building's roof and a floor are well insulated and only a wall effect is considered.

For design purposes, only one south wall and a quarter of the total room air mass are considered. Examining a south wall will be a reasonable assumption because the buildings modelled are all located in the northern hemisphere and the south wall will allow the effects of the solar flux in January and August to be studied.

The system is considered as one-dimensional. The heat transfers in the Y and Z directions are assumed to be negligible, and the heat flow occurs principally in the direction perpendicular to the surface of the wall (X-direction). Neglect of heat flow in the Y and Z directions should not significantly affect the applicability of the solution.

Under this study there is no heat generation within the wall, and the energy balance, after some manipulation, yields:

$$\partial^2 T/\partial x^2 = (1/\alpha)\partial T/\partial t \tag{1}$$

Two corresponding boundary conditions to the above linear, second-order, partial differential equation are:

$$-k\partial T/\partial x\,(x=0) = \hat{a}S^* + h_e\,(T_\infty - T_0) \tag{2}$$

$$-k\partial T/\partial x\,(x=L) = -h_i\,(T_A - T_L) \tag{3}$$

The initial condition for the wall temperature is expressed in polynomial form as:

$$T\,(x,\,0) = \sum_{n=0}^{4} a_n x^n \tag{4}$$

Approximating the initial condition in polynomial form provides the initial condition whenever the auxiliary energy source is activated or deactivated. If the actual wall temperature profile were to be used condition, it would be impossible to obtain an analytical solution. Therefore, it is necessary to simplify the initial condition in a form which captures all "essential" information of the problem.

Having a well-approximated initial condition, which is very close to the actual initial wall temperature profile, is important because the initial condition must be reset whenever the auxiliary energy source (Q) switches on and off.

The coefficients in equation (4) are determined as follows:

1) The actual wall temperature at x =0 is the same as T (0, *t**) in equation (4), where *t** is the time at which the controller function changes.

2) The actual wall temperature at x =L is the same as T (L, *t**) in equation (4).

3) Internal energy is conserved in the wall (proportional to the integral of the wall temperature from x =0 to x =L).

Five equations are necessary to obtain the five coefficients, through . Three equations are explicit from the above three statements. Two more equations are formulated using the least-squares method (Gerald, 2005).

$$S = \sum_{i=0}^{M} (Y_i - y_i)^2 \tag{4}$$

where Y_i represents the actual temperature data and y_i represents the assumed profile for the initial condition, containing two unknown coefficients, a_3 and a_4.

A minimum of s is achieved through proper choice of the parameters a_3 and a_4. At the minimum of s, the two partial derivatives $\partial s/\partial a_3$ and $\partial s/\partial a_4$ are both zero.

The energy balance for the room air temperature including heat transfer from the inside surface of the wall, infiltration loss, and auxiliary heat input Q, is:

$$C_A dT_A/dt = -h_i A (T_A - T_L) - C_A' I (T_A - T_\infty) + Q \tag{6}$$

$$C_A = (\rho C_v)_A V_A \tag{7}$$

$$C_A' = (\rho C_p)_A V_A \tag{8}$$

$$I' = C_A I / C_A \tag{9}$$

The parameters, h_i, h_e, CA, CA′ and I are assumed constant.

The corresponding initial condition to equation (6) is as follows:

$$T_A(0) = T_i \tag{10}$$

There exists a coupling between wall and room air temperatures, and the two sets of equations must be solved simultaneously.

Weather data for four cities in the United States are used in this study. Those cities under study are Albuquerque, NM; Miami, FL; Santa Maria, CA; and Washington, D.C. Two of the cities, Albuquerque and Washington D.C., have four distinct seasons, while Santa Maria experiences mild weather conditions year round. Miami weather is the hottest of the four cities studied, and houses need to be cooled nearly year round.

TMY (Typical Meteorological Year) weather data files are used to obtain hourly values of the solar flux and ambient temperature. The monthly average hourly values, x_i (X is used for either temperature, direct normal horizontal radiation), are given as:

$$x_i = (1/N_k) \sum_{j=1}^{N_k} x_{ij} \tag{11}$$

where X_{ij} is the temperature at a given hour for each day of a particular month, read from TMY data files. In this expression, i indicates the hour and k indicates the particular month, and j varies over N_k -- the total number of days in month "k".

After obtaining monthly average hourly direct normal radiation and total horizontal radiation, solar flux for the vertical wall is calculated. No shading on the wall is considered in this study.

The calculation method for the solar flux is given from the reference of Duffie et al. (2000):

Liu et al. (1961) suggest values of diffuse ground reflectance of 0.2 when there is no snow, and 0.7

when there is a fresh snow cover. For design purposes, as mentioned earlier, the wall is modelled as south facing and vertical. In the case of January in Washington D.C., the solar flux is calculated for both values of ground reflectances (0.2 and 0.7). To represent an "average" snow cover, these results are averaged to yield the weather data used in this analysis.

All other cities employ a ground reflectance of 0.2 for both August and January. Twenty-four discrete data points are converted to continuous form with the use of a Fast Fourier Transform. Brigham (2004) discusses the use of a Fast Fourier Transform method for this purpose.

Hence, the weather data input to the analytical model is finally represented in the following form:

$$S^*(t) = b_0 + \sum_{i=1}^{11} [b_i \cos(w_i t + \Phi_i) + c_i \sin(w_i t + \Phi_i)] \quad (12)$$

$$T_\infty(t) = d_0 + \sum_{i=1}^{11} [d_i \cos(w_i t + \Phi_i) + e_i \sin(w_i t + \Phi_i)] \quad (13)$$

where b_0 is the DC component of the solar flux and d_0 is the DC component of the ambient temperature.

Twenty-four processed hourly weather data points for Washington D.C. (+ points in Fig. 1 and Fig. 2) and a continuous graph obtained from the Fourier series fit to the data are shown in Fig. 1 and Fig. 2. Agreement between processed hourly weather data points and fitted data points based on equations (12) and (13) is excellent.

Table 2 gives the individual properties of materials used in this study, obtained from ASHRAE handbook (1981) and Holman (1997).

Table 3 lists the wall thermal resistances of each layer for each of the four houses. If there exists two parallel different components in one layer, the

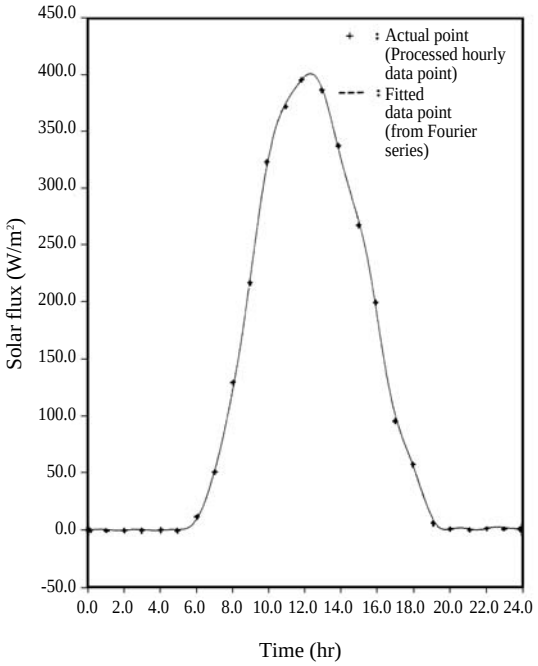

Fig. 1. Comparison of actual points and fitted data of solar flux (Washington D.C., August)

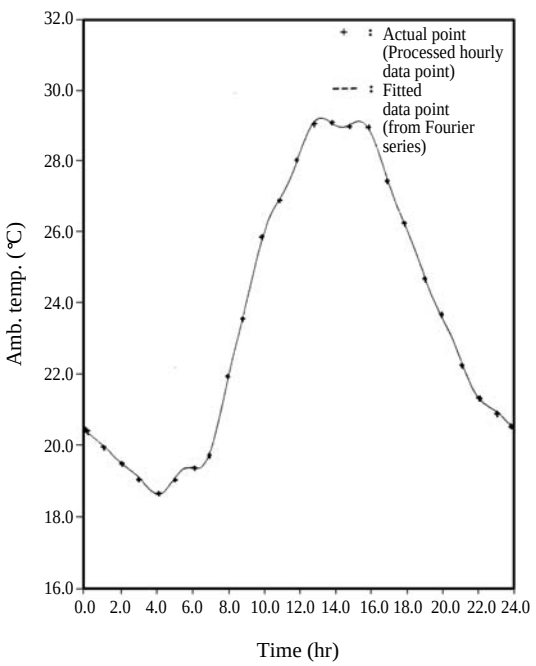

Fig. 2. Comparison of actual points and fitted data of ambient temperature (Washington D.C., August)

Table 2. Properties of building materials

	k (W/m°C)	ρ (kg/m^3)	Cp (J/kg°C)
Gypsum board	0.165	800.0	1089
Plaster	0.170	800.0	1089
2-core hollow concrete block	0.930	1680.0	921
Face brick	1.320	2080.0	796
Wood stud	0.116	640.0	1380
Plywood	0.150	544.0	1214
Wood furring strip	0.100	500.0	2500
Blanket insulation	0.046	32.0	1000
Extruded polystyrene insulation	0.033	50.0	1214
Perlite insulation	0.053	100.0	1089
Air	0.026	1.2	1006

combined resistance is calculated as:

$$R_{com} = R_a R_b / (aR_b + bR_a) \tag{14}$$

where R_{com} is the combined resistance of R_a and R_b, and a and b are proportionate areas for the two parallel components, respectively. Isothermal planes are assumed to exist at both surfaces on either side of the layer.

Control function is desired to maintain comfort inside the house. In order to accomplish this practically, the rate of supply of heat to the building is regulated by a controller. Two types of control mechanisms are chosen for investigation. One is a simple 'on-off' controller; the other is a proportional controller.

The rate of supply of heat produced by the proportional controller is modelled as proportional to the difference between the set-point temperature and the room air temperature as:

$$Q = \Gamma (T_S - T_A) \tag{15}$$

The non-dimensionalized variables are defined as:

$$x' = x/L \tag{16}$$

$$t' = at/L^2 \tag{17}$$

$$\theta = T/\Delta T \tag{18}$$

$$\Delta T = T_S - \overline{T_\infty} \tag{19}$$

where $\overline{T_\infty}$ is an average ambient temperature over a 24 hour period.

Equation (1) and boundary conditions, equations (2) and (3), and equation (6) for the room air temperature can be rearranged as follows:

$$\partial^2\theta/\partial x'^2 = \partial\theta/\partial t' \tag{20}$$

$$-\partial\theta/\partial x'(x'=0) = \hat{a}LS^*/(k\Delta T) + h_e L\,(T_\infty/\Delta T - \theta(x'=0))/k \tag{21}$$

$$\partial\theta/\partial x'(x'=1) = -h_i L\,(T_A/\Delta T - \theta(x'=1))/k \tag{22}$$

$$(1/\Delta T)dT_A/dt' = -h_i A L^2\,(T_A/\Delta T - \theta(x'=1))/(\alpha C_A) - L^2 I'\,(T_A/\Delta T - T_\infty/\Delta T)/\alpha + QL^2/(C_A\alpha\Delta T) \tag{23}$$

The analytical solution is seen to include some important terms such as the Fourier number and the Biot number, and consequently, the solution can be represented in non-dimensional parameterized form as follows:

$$T = T(x', t', Fo, Bi_1, Bi_2, \hat{a}LS^*/(k\Delta T), \Delta T_A/\Delta T, QL^2/(C_A\alpha\Delta T), \text{initial conditions}) \tag{24}$$

where the two Biot numbers are:

$$Bi_1 = h_e L/k \tag{25}$$

$$Bi_2 = h_i L/k \tag{26}$$

Table 3. Thermal resistances for four houses

Thermal resistance (m^2°C/W)	House			
	#1	#2	#3	#4
R1	0.079	0.079	0.079	0.076
R2	1.694	1.372	0.538	0.218
R3	0.107	0.231	0.218	1.679
R4	-	0.110	-	0.077
R5	-	0.077	-	-
R_{total}	1.880	1.8369	0.835	2.050

Laplace transform solution

The methods used to obtain expressions for the wall temperature profile and room air temperature trajectory are presented. Several methods were considered to solve the problem. The first attempt was to divide the original equation into three sub-problems because the problem was linear and the sub-problems were each simpler to solve. The solutions to these simpler problems can then be super-imposed to obtain the complete solution of the original problem (Myers, 2001).

The first sub-problem dealt with the weather conditions, the second one incorporated the initial condition, and the third one dealt with the auxiliary energy source. It seemed to be a very good approach, but unfortunately the attempt was seriously flawed because the second sub-problem was not a Sturm-Liouville eigenvalue problem.

Next, the Laplace transform approach was adopted, and proved to be successful although the inversion from the Laplace domain to the real time domain was extremely complicated due to higher order poles.

In this study, there exists a pole of order three at $s=0$, and the use of the Complex Inversion Theorem is extremely complicated and cumbersome. The Laplace transform solution technique, however, is successfully applied to the problem under study, and the inversion from the Laplace domain to the time domain is accomplished using the Complex Inversion Theorem using Bromwich contour (Carslaw et al., 1959).

The form of the wall temperature as a function of time is:

$$\begin{aligned} T(x,t) = & \sum_{m=1}^{\infty}[(A_m/C_m)\mathrm{EXP}(-\alpha\eta_m^2 t)\cos(\eta_m x) \\ & +(B_m/C_m)\mathrm{EXP}(-\alpha\eta_m^2 t)\sin(\eta_m x)] \\ & +a_0+a_1x+a_2x^2+a_3x^3+a_4x^4+2\alpha a_2 t \\ & +12\alpha^2 a_4 t^2+6\alpha a_3 xt+12\alpha a_4 x^2 t \\ & +(1/2)[(N_1/D)(t^2+tx^2/\alpha+x^4/(12\alpha^2)) \\ & +(N_1'/D)(2t+x^2/\alpha)+N_1''/D-D''N_1/D^2 \\ & -(2D'/D^2)[(t+x^2/(2\alpha))N_1+N_1'] \\ & +2D'^2N_1/D^3+(N_2/D)(t^2x+tx^3/(3\alpha) \\ & +x^5/(60\alpha^2))+(N_2'/D)(2tx+x^3/(3\alpha)) \\ & +(N_2''x/D-D''N_2x/D^2-(2D'/D^2)[(tx \\ & +x3/(6\alpha))N_2+N_2'x]+2D'^2N_2x/D^3] \\ & +\sum_{i=1}^{11}[x_{1i}(x)\cos(w_i t)+x_{2i}(x)\sin(w_i t)] \end{aligned} \quad (27)$$

The form of the room air temperature as a function of time is:

$$\begin{aligned} T_A(t) = & \sum_{m=1}^{\infty}[(A_m/D_m)\mathrm{Mcos}(\eta_m L)\mathrm{EXP}(-\alpha\eta_m^2 t) \\ & +(B_m/D_m)\mathrm{Msin}(\eta_m L)\mathrm{EXP}(-\alpha\eta_m^2 t) \\ & +((a_{32}+a_{36})/c_{33}-c_{39}+c_{42}+T_i)\mathrm{EXP}(-\beta t) \\ & +(1/2)[F_6/F_1-(F_4D''+2F_5F_2)/(F_1)^2 \\ & +2F_4(F_2)^2+F_9/F_1-(F_7F_3+2F_8F_2)/(F_1)^2 \\ & +2F_7(F_2)^2/(F_1)^3]+\sum_{i=1}^{11}[(x_{3i}+F_{10})\cos(w_i t) \\ & +(x_{4i}+F_{11})\sin(w_i t)]+(Ma^*/\beta-Mc^*/\beta^2)t \\ & +Mc^*t^2/(2\beta)+c_{39} \end{aligned} \quad (28)$$

where η_m is the m^{th} root of the characteristic equation:

$$\tan(L\eta_m)=[-\eta_m(c_{14}s_m+c_{15})]/(c_{16}s_m^2+c_{17}s_m+c_{18}) \quad (29)$$

Results and discussion

The values of wall temperature and room air temperature calculated from the analytical solution are presented. Energy consumption loads are calculated for each house under varying weather conditions. Indoor comfort is discussed for an on-off controller and a proportional controller.

The weather conditions produce a forced response that is evaluated without any auxiliary energy source. Because these forcing functions are in the form of a Fourier series, the nature of the room air temperature (i.e. the forced response) is

sinusoidal, as illustrated in Fig. 3.

The heat wave penetration phenomenon is now examined further, as shown in Fig. 4, which present temperature profiles plotted every 4 hours in time.

As the thermal wave penetrates the walls, the amplitude is seen to progressively diminish. House #1 again shows the largest temperature variation at x = L, causing the largest room air temperature swing, Houses #2 and #4, which have high time delays, show the smallest temperature variation at x = L. Houses #2 and #4 (masonry wall with insulation) maintain almost constant temperature. Significant energy is stored in and released from the masonry walls. This serves to minimize the room air temperature fluctuations (Mazria, 1999).

Fig. 5 show the daily room air temperature variation in one of four cities for all four houses. Since the on-off controller is functioning, the room air temperature lies mostly inside the dead band of the controller. The upper and a lower bounds of the dead band are taken as 23 and 21, respectively.

It is interesting to note that the weather interacts with the inside air, evident from the variation in cycle rate over the day. Examining Fig. 5, one observes that the interaction is primarily through the wall as opposed to through infiltration. This is evident because the cycling rate for house #3,

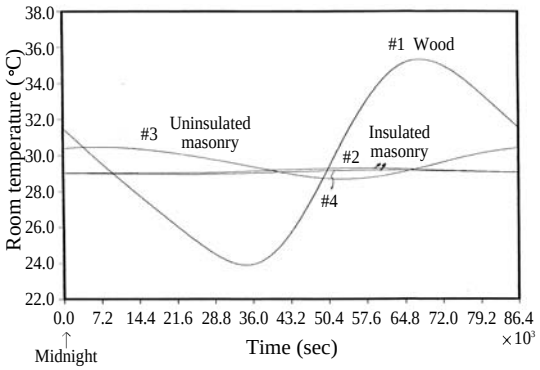

Fig. 3. Room air temperature variation for four simulated houses (free response, Albuquerque, August)

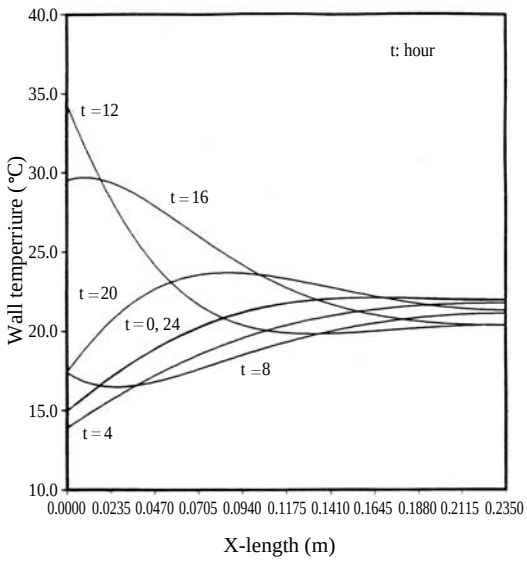

Fig. 4. Wall temperature profile, free response, at seven different times (house #3, Santa Maria, August)

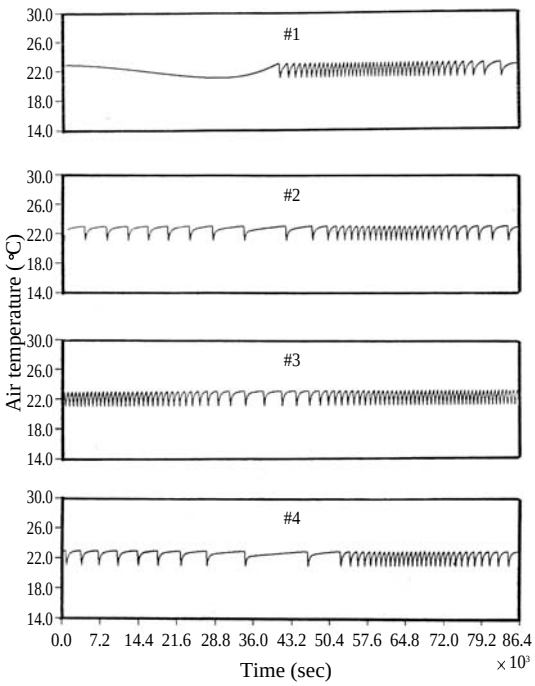

Fig. 5. Room air temperature variation for four house (on-off controller, Washington D.C., August)

Table 4. Energy consumption loads (on-off controller)

City, month, house #	Energy consumption load (MJ/day)	City, month, house #	Energy consumption load (MJ/day)
AA1	4.210	SA1	1.463
AA2	3.576	SA2	0.068
AA3	9.011	SA3	0.519
AA4	4.022	SA4	0.143
AJ1	7.496	SJ1	4.248
AJ2	7.384	SJ2	4.125
AJ3	16.110	SJ3	7.555
AJ4	8.002	SJ4	4.755
MA1	5.246	WA1	3.455
MA2	4.534	WA2	2.797
MA3	11.739	WA3	6.997
MA4	4.965	WA4	3.132
MJ1	2.203	WJ1	10.092
MJ2	1.498	WJ2	9.521
MJ3	3.433	WJ3	22.564
MJ4	0.361	WJ4	10.188

which experiences similar infiltration to the other houses, shows little variation in cycle rate.

Again, the lightweight house (#1) shows a higher amplitude of the wall temperature variation than the heavyweight houses (#2, #3 and #4). The interaction of the control and the weather is apparent in the average variation. Energy loads are calculated and listed in Table 4. Abbreviations used to simplify display in the Table are (1) first column: city-- A, M, S and W for Albuquerque, Miami, Santa Maria, and Washington D.C., (2) second column: month -- A, J for August and January, and (3) third column: house numbers -- #l, #2, #3 and #4.

Fig. 5 shows plots made using a basis of 400 W, regardless of houses or months. However, different cycling phenomena occur when using different Q´s for the same house and weather conditions.

Results are now presented for a proportional controller The output of the auxiliary energy source in this case is proportional to the difference

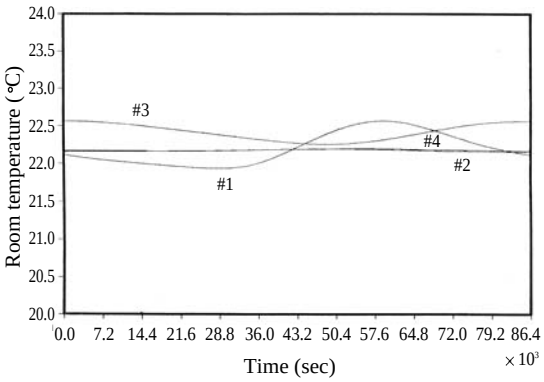

Fig. 6. Room air temperature variation for four houses (proportional controller, Albuquerque, August)

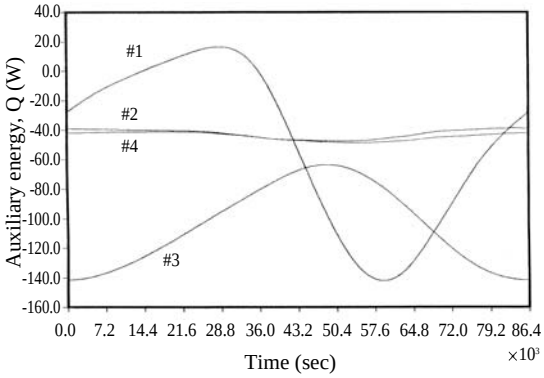

Fig. 7. Auxiliary energy input vs. time (proportional controller, Albuquerque, August)

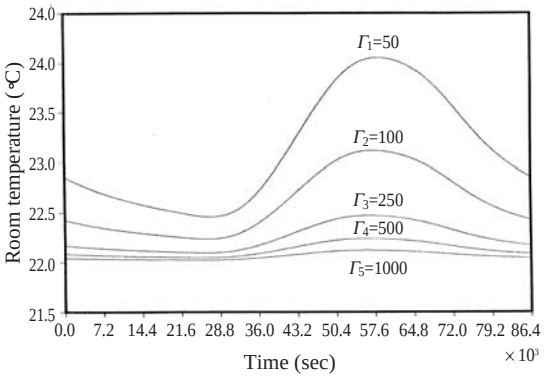

Fig. 8. Room air temperature variation for five different *Γ*´s (proportional controller, house #1, Miami, August)

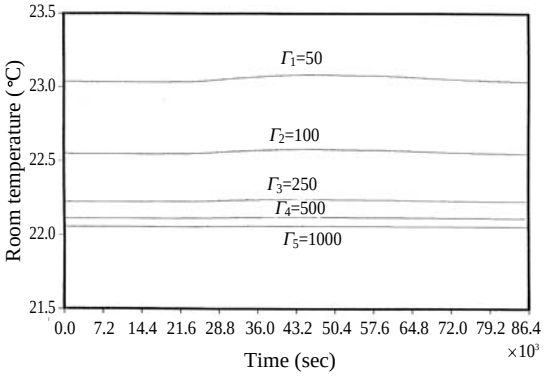

Fig. 9. Room air temperature variation for five different Γ's (proportional controller, house #4, Miami, August)

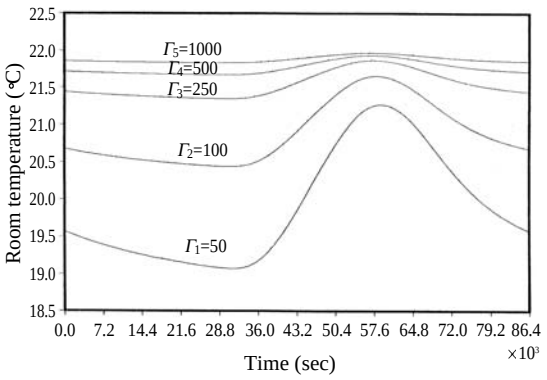

Fig. 10. Room air temperature variation for five different Γ's (proportional controller, house #1, Washington D.C., January)

between the actual room air temperature and the set-point temperature as mentioned in equation (15).

Several values of Γ are tested to obtain room air temperature trajectories, When too small a value of Γ is used, the room air temperature lies between the comfort range and the sol-air temperature. This occurs because Q is not large enough to heat (or cool) the room air to approach T_s. Appropriate values of Γ are determined after several trials for all four houses.

In Fig. 6, a sample plot of the room air temperature trajectories over a daily period is presented

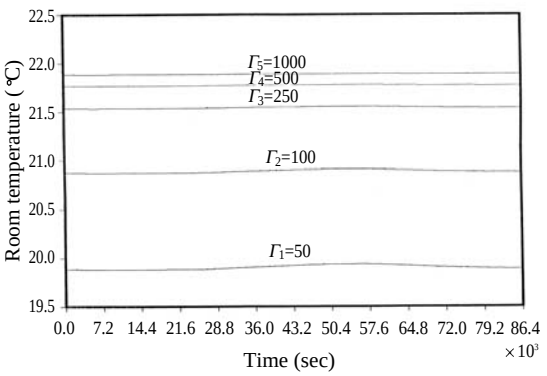

Fig. 11. Room air temperature variation for five different Γ's (proportional controller, house #4, Washington D.C., January)

for the four houses for August in Albuquerque. Fig. 7 also shows the auxiliary energy input versus time, which is the scaled image of Fig. 6 reflected about T_s because of the nature of equation (15). The value of Γ is 250W/℃ in Fig. 6 and Fig. 7.

Fig. 8 and through Fig. 9 show the room air temperature variation for five different Γ's. Houses #1 and #4 are chosen to compare the lightweight and heavyweight walls with insulation, and Miami in August and Washington D.C. in January are used for weather conditions because these two cities experience the extremes in hot and cold weather, respectively.

A small Γ, such as 50 W/℃, results in temperatures far removed from the set-point temperature, while using a large Γ makes the room air temperature very close to T_s.

A high temperature swing is again observed in house #1. This swing increases as decreases. However, no noticeable temperature swing is observed in house #4 even though Γ is small due to the high thermal mass. Table 5 shows all these comparisons. The comfort level increases as Γ increases, but this results in greater energy input.

Table 5. Comparison when different Γ's are used for proportional control

City, month, house #	Γ (W/°C)	Load (MJ)	$\overline{T}_A$	$\overline{T}_0$	$\overline{T}_L$	σT_A	σT_0	σT_L	σT_S
			℃				℃		
MA1	50	4.88	23.13	31.72	23.59	0.56	6.51	0.80	1.26
	100	5.18	22.60	31.70	23.08	0.31	6.51	0.57	0.68
	250	5.38	22.25	31.69	22.75	0.13	6.51	0.41	0.28
	500	5.45	22.13	31.69	22.64	0.07	6.51	0.35	0.14
	1000	5.49	22.06	31.69	22.58	0.03	6.51	0.32	0.07
MA4	50	4.56	23.06	31.28	23.49	0.02	5.10	0.02	1.06
	100	4.83	22.56	31.26	23.02	0.01	5.10	0.01	0.56
	250	5.02	22.23	31.25	22.71	0.01	5.10	0.01	0.23
	500	5.08	22.12	31.25	22.60	0.00	5.10	0.01	0.12
	1000	5.11	22.06	31.25	22.54	0.00	5.10	0.01	0.06
WJ1	50	5.10	19.89	5.08	19.11	0.74	8.87	1.05	2.24
	100	9.67	20.88	5.11	20.04	0.41	8.87	0.75	1.19
	250	10.05	21.54	5.13	20.66	0.17	8.87	0.54	0.50
	500	10.18	21.76	5.14	20.88	0.09	8.87	0.46	0.25
	1000	10.25	21.88	5.14	20.99	0.05	8.87	0.42	0.13
WJ4	50	9.05	19.91	4.49	19.10	0.02	6.81	0.02	2.10
	100	9.60	20.89	4.52	20.03	0.01	6.81	0.02	1.11
	250	9.96	21.54	4.54	20.65	0.01	6.81	0.01	0.46
	500	10.08	21.77	4.55	20.87	0.00	6.81	0.01	0.23
	1000	10.15	21.88	4.55	20.98	0.00	6.81	0.01	0.12

Conclusions

The preceding work has led to the following conclusions: There is a significant wall mass effect on the thermal performance of a house in mild weather conditions. This effect is due to the thermal wave (due to ambient variability) penetrating the structure, and interacting in a non-linear fashion with the auxiliary energy system controller. This interaction has been observed to occur only when the thermal wave in the situation of free response causes the room air temperature to cross the dead band. Houses of heavyweight construction with insulation (houses #2, #4) show the highest contort level in mild weather areas. This is true both in terms of room air temperature, and mean radiant temperature as both fluctuate very little. A proportional controller provides the highest comfort levels in comparison with houses using an on-off controller. Comfort can be increased by using a smaller dead band in the on-off controller; however this leads to more rapid cycling (and therefore inefficiency) of the auxiliary energy source. As far as energy consumption loads are concerned, there is no big difference between the proportional controller and the on-off controller. No noticeable energy load difference is observed when varying the heating rate as long as the auxiliary energy unit is large enough to cause the temperature to exceed the dead band. Note, however, that energy inefficiencies in the heating plant due to cycling are not considered in this study. Using an optimum heating rate will be important in practice because high cycling decreases heating plant efficiency. Finally, it appears that both mass and wall insulation are important factors in the thermal performance of buildings in general, but their relative merits should be decided in each house by a strict analysis of the house layout, weather conditions, site location.

References

ASHRAE handbook of 1981 fundamentals, 1982. American Society of Heating, Refrigerating and Air-Conditioning Engineers, Inc., 21.1 - 21.9.

Brigham, E.O., 2004. The fast Fourier transform. Prentice Hall, Inc., 25 - 150.

Buffington, D.E., 1995. Heat gain by conduction through exterior walls and roofs-transmission matrix method. ASHRAE Transactions 81, Part 2, 89 - 101.

Burch, D. M., D.F. Kritz and R.S. Spain, 1984. The effect of wall mass on winter heating loads and indoor comfort-an experimental study. ASHRAE Transactions 90, Part 1, 94 - l21.

Burch, D.M., S.A. Malcolm and K.L. Davis, 1984. The effect of wall mass on the summer space cooling of six test buildings. ASHRAE Transactions 90, Part 1, 5 - 20.

Carslaw, H.S. and J.C. Jaeger, 1959. Conduction of heat in solids. Oxford Press, Great Britain, 92 - 326.

Crall, G.C., C.D. Jones, C.F. Sepsy and J.W. Jones, 1995. A computer simulation and validation of a building heating, ventilating and air conditioning system. ASHRAE Transactions 81, Part 1, 506 - 5l8.

Duffie, J.A. and W.A. Beckman, 2000. Solar engineering of thermal processes, John Wiley & Sons, Inc., 28 - 110.

Gerald, C.F., 2005. Applied numerical analysis. Addison-Wesley Publishing Company, 45 - 186.

Goodwin, S.E. and M.J. Catani, 1979. The effect of mass on heating and cooling loads and on insulation requirements of buildings in different climates. ASHRAE Transactions 85, Part 1, 869 - 884.

Holman, J.P., 1997. Heat transfer. Prentice Hall, Inc., 635 - 654.

Hopkins, V., G. Gross and D. Ellifritt, 1979. Comparing the thermal performance of buildings of high and low masses. ASHRAE Transactions 85, Part 1, 885 - 902.

Kondepudi, S.N., 1986. A study on the effect of wall mass of buildings on the thermal response of buildings. M.S. Thesis, Mechanical Engineering Department, Colorado State University, 10 - 150.

Liu, B.Y.H. and R.C. Jordan, 1961. Daily insolation on surfaces tilted toward the equator. ASHRAE Journal, 3 (1), 53 - 59.

Mazria, E., 1999. The passive solar energy book. Rodale Press, 35 - 65.

Mitalas, G.P. and D.G. Stephenson, 1967. Room thermal response factors. ASHRAE Transactions 73, Part 1, III.2.1 - III.2.10.

Mitalas, G.P., 1968. Calculation of transient heat flow through walls and roofs. ASHRAE Transactions 74, Part 2, 182 - 188.

Myers, G.E., 2001. Analytical methods in conduction heat transfer. McGraW-Hill, Inc., New York, 175 - 205.

Rudoy, W. and R.S. Dougall, 1979. Effects of the thermal mass on heating and cooling load in residences. ASHRAE Transactions 85, Part 1, 903 - 9l7.

Tape Deck #9734, 1998. Typical meteorological year (TMY). Sandia Report, 7 - 120.

Zabinski, M.P. and L. LoVerme, 1974. Fuel consumption in residential heating at various thermostat settings. ASHRAE Journal, Vol. 16, 67 - 70.

2010년 1월 8일 접수
2010년 1월 26일 1차 수정
2010년 2월 1일 수리